

Electronic Supplementary Information

Defect-Engineered Porphyrinic Metal-Organic Framework Nanoparticles for Targeted Multimodal Cancer Phototheranostics

Chenyuan Wang ^a, Chuxiao Xiong ^a, Zhike Li ^a, Liefeng Hu ^a, Jianshuang Wei^b and Jian Tian^{*a}

^aKey Laboratory of Combinatorial Biosynthesis and Drug Discovery (MOE), School of Pharmaceutical Sciences, Wuhan University, Wuhan 430071, China.

^b Collaborative Innovation Center for Biomedical Engineering, Wuhan National Laboratory for Optoelectronics-Huazhong University of Science and Technology, Wuhan, Hubei 430074, China.

* Corresponding authors.

E-mail address: jian.tian@whu.edu.cn

Content

Instruments and Materials.....	3
Synthesis of H ₂ TCPP	3
Synthesis of cypate	4
Synthesis of PC _X -MOFs	6
Cypate stability assay.....	6
UV-Vis absorbance curves of cypate and H ₂ TCPP.....	6
Preparation of PC ₂₀ -MOFs-FA	6
<i>In vitro</i> stability assay	6
Photothermal effects of PC ₂₀ -MOFs-FA.....	6
Photodynamic effects of PC ₂₀ -MOFs-FA	7
Cytotoxicity assessment.....	7
Hemolysis assay.....	8
<i>In vivo</i> biocompatibility.	8
Cellular uptake.....	8
<i>In vitro</i> PDT and PTT experiments.....	9
Calcein-AM/PI double Staining.....	9
Construction of 4T1 tumor-bearing mice.....	9
<i>In vivo</i> multimodal imaging	10
<i>In vivo</i> phototherapy	10
Statistical analysis.....	11

Instruments and Materials

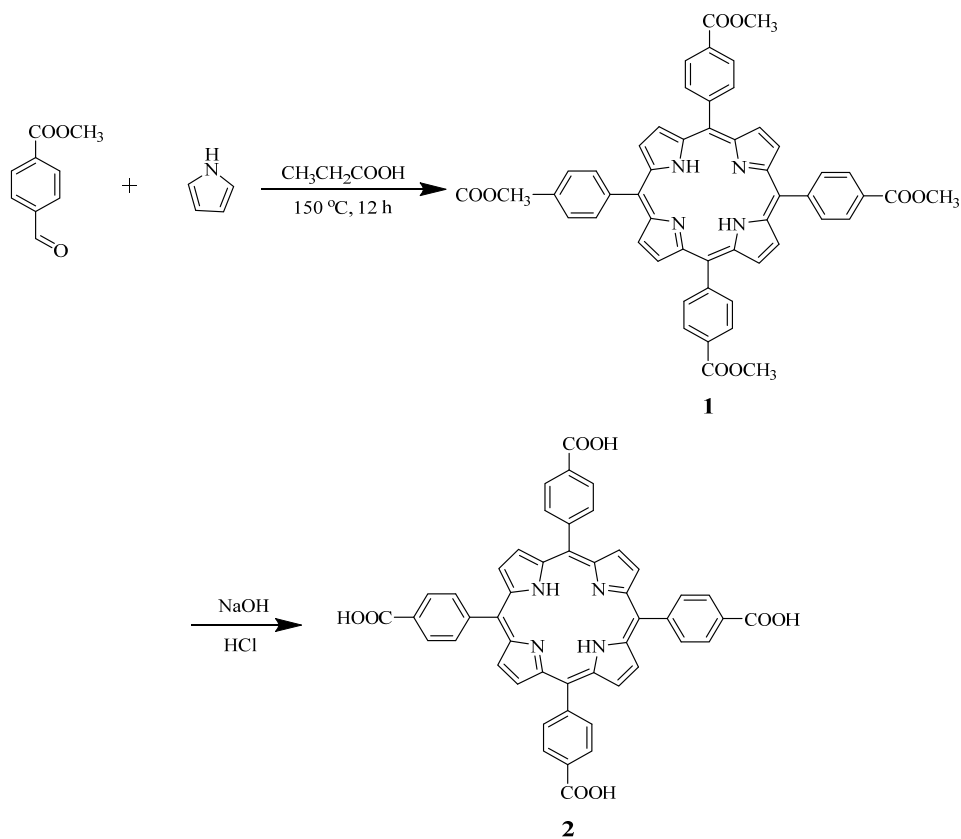
Transmission electron microscope (TEM) images were acquired from HITACHI H-7000FA TEM. The UV-visible absorption spectrum was measured with a Shimadzu UV-2600 spectrophotometer. The hydrodynamic diameter and zeta potential were observed by Dynamic light scattering (DLS) particle size analyzer (Malvern Nano-ZS90). Powder X-ray diffraction (PXRD) patterns were obtained on a Rigaku MiniFlex600 Focus Powder Diffractometer with Cu K α line focused radiation. BET (Brunauer-Emmett-Teller) surface area analysis was performed with a Micromeritics ASAP 2420 analyzer. Laser confocal fluorescence microscope (CLSM) images were collected by Carl Zeiss NOL-LSM 710. In vivo near-infrared fluorescence images were captured using live animal imaging system (Suzhou Yingrui Optical Technology Co.). Inductively coupled plasma mass spectrometry (ICP-MS) was measured by an Analytik Jena inductively coupled plasma mass spectrometer. Unless otherwise specified, all reagents were analytical reagents purchased from commercial companies without further purification. Folate acid and DPBF were provided by Energy Chemical (Shanghai, China). 3-(4,5-Dimethyl-2-thiazolyl)-2,5-diphenyl -2H-tetrazolium bromide (MTT) and Calcein-AM/PI Double Stain Kit were purchased from Sigma-Aldrich (Shanghai, China). 2',7'-dichlorodihydrofluorescein diacetate (DCFH-DA) was purchased from Beyotime (Shanghai, China). All cell lines used in this project were from the Chinese Type Culture Collection (Wuhan University). Cell cultures were obtained from Gibco Invitrogen, including phosphate buffered saline (PBS), Dulbecco's modified Eagle medium (DMEM), penicillin, streptomycin, and fetal bovine serum (FBS).

Synthesis of H₂TCPP

The tetrakis(4-carboxyphenyl)porphyrin (H₂TCPP) ligand was synthesized based on the previous literature¹. Methyl p-formylbenzoate (6.9 g, 0.042 mol) was dissolved in

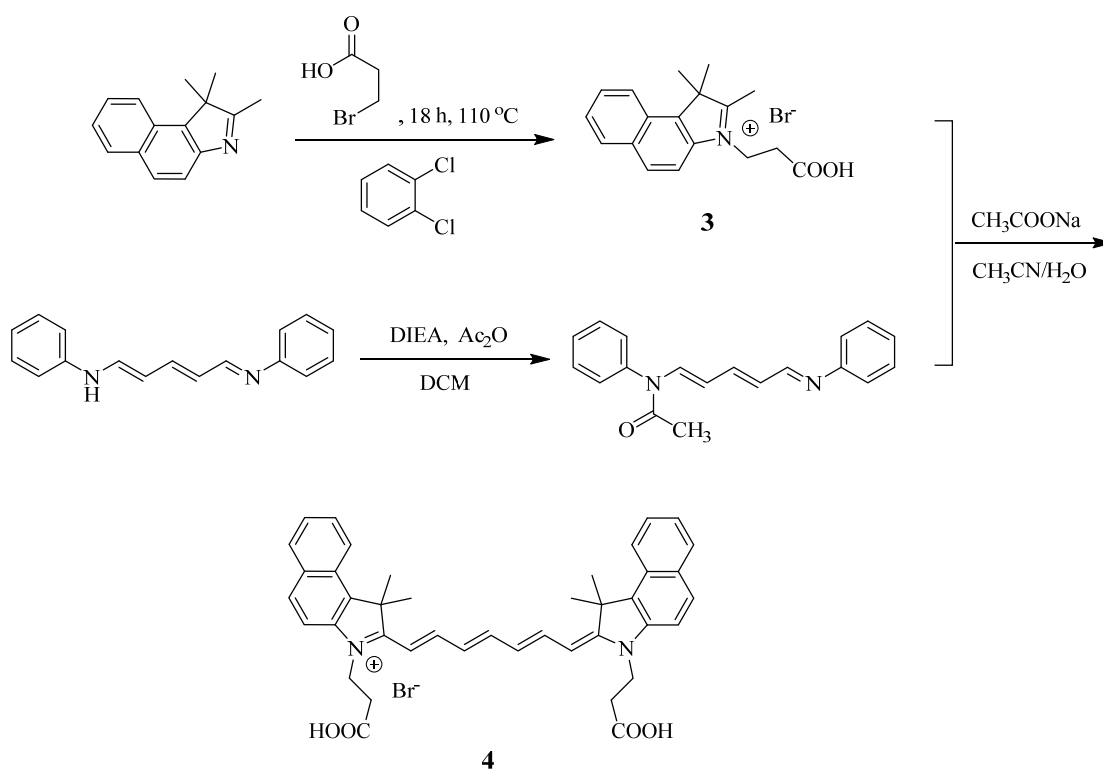
propionic acid (100 mL) and then pyrrole (3.0 mL, 0.043 mol) was added dropwise. The reaction was refluxed for 12 h and then cooled to room temperature. The precipitate was collected by suction filtration and washed with methanol, ethyl acetate and THF respectively. Purple powder was obtained after being dried in oven overnight (Compound 1). $^1\text{H NMR}$ (400 MHz, CDCl_3): δ (ppm) = 8.82 (s, 8H), 8.45 (d, 8H), 8.29 (d, 8H), 4.11 (s, 12H), -2.82 (s, 2H).

Compound 1 (1.5 g, 1.78 mmol) was dissolved in a mixed solution of 100 mL THF/MeOH (v/v = 1/1), then 25 mL of NaOH (2.4 g, 60 mmol) aqueous solution was added, and the mixture was refluxed for 12 h. After the reaction system was cooled to room temperature, the organic solvent was removed by evaporation under reduced pressure. An appropriate amount of water was added to the reaction solution, and then 1 M HCl was used to acidify the solution until the product precipitated completely. The precipitate was collected by filtration, washed with water and dried in vacuum oven to obtain H_2TCPP (Compound 2). $^1\text{H NMR}$ (400 MHz, $\text{DMSO-}d_6$): δ (ppm) = (s, 8H), 8.35 (m, 16H), -2.94 (s, 2H).



Synthesis of cypate

The synthesis of cypate was divided into two steps². The first step is to synthesize 1,1,2-trimethyl-[1H]-benz[e]indole-3-propionic acid. Mixture of 1,1,2-trimethyl-[1H]-benzo [e] indole (40.0 g, 0.19 mol) and 3-bromopropionic acid (40.0 g, 0.26 mol) in 1,2-dichlorobenzene (200 mL) was heated to 110 °C and stirred for 18 h. After the reaction was cooled to room temperature, the precipitate was collected by filtration. In order to remove unreacted materials, it was ground in dichloromethane (DCM) for 15 min, and then transferred to a vacuum drying oven to obtain 1,1,2-trimethyl [1H]-benzo [e] Indole-3-propionic acid (Compound 3 in the reaction formula, 0.94g, yield: 52.6%).
¹H-NMR (400 MHz, DMSO-*d*₆): δ (ppm) = 8.37 (d, 1H), 8.29 (d, 1H), 8.23-8.16 (m, 2H), 7.81-7.71 (m, 1H), 4.77 (t, 2H), 3.04 (t, 2H), 2.96 (s, 3H), 1.75 (s, 6H).



Synthesis of cypate: Glutaconaldehyde dianil monohydrochloride (284 mg, 1 mmol) and N, N-diisopropylethylamine (DIEA) (351 μL, 2.01 mmol) were dissolved in 2 mL DCM. The resulting suspension was placed in an ice-water bath and stirred, and then DCM (0.5 mL) solution of acetic anhydride (Ac₂O, 123 μL, 1.18 mmol) was added dropwise. The resulting clear solution was stirred for 1 hour and added dropwise with 1,1,2-trimethyl-[1H]-benz[e]indole-3-propionic acid (Compound 3, 0.82 g, 2.27 mmol)

obtained in the first step and sodium acetate (0.32, 3.9 mmol) in acetonitrile / water (9.5 / 0.5 mL). The mixture was refluxed for 16 hours, cooled, filtered, washed with acetonitrile, 5% hydrochloric acid solution and ether, and dried in vacuo to get cypate (Compound 4, 0.5 g, 70.8%). ¹H NMR (400 MHz, DMSO-*d*₆): δ (ppm) = 12.66 (br, 2H), 8.26 (d, 2H), 8.08-7.97 (m, 6H), 7.86-7.73 (m, 3H), 7.65 (t, 2H), 7.5 (t, 2H), 6.60 (t, 2H), 6.47 (d, 2H), 4.43 (t, 4H), 2.77 (t, 4H), 1.91 (s, 12H).

Synthesis of PC_X-MOFs

ZrOCl₂·8H₂O (15 mg, 0.0465 mmol), H₂TCPP (4 mg, 0.0052 mmol), benzoic acid (140 mg, 1.15 mmol), and a certain amount of cypate (5 mg-40 mg, 0.0080 mmol-0.064 mmol) were dissolved in 5 mL DMF. The mixture was put in a 20 mL glass vial with sealed cap and reacted in an oven at 90 °C for 5 h. After cooling to room temperature, the purple precipitate was collected by centrifugation (11000 rpm, 30 min) and washed thoroughly with hot DMF solvent three times to remove unreacted cypate before lyophilization.

Cypate stability assay

Equal amounts of PC₂₀-MOFs and Cypate@PCN-224 were dialyzed in dialysis tubing by methanol solution (the molecular weight cut-off was 6000). The dialysate was detected by UV-vis spectrophotometer every 12 h.

UV-Vis absorbance curves of cypate and H₂TCPP

Cypate solutions with a concentration gradient from 0.375-12 μg mL⁻¹ in DMSO/water (v/v, 1/99) were prepared, and the absorbance spectra from 700-800 nm were recorded. H₂TCPP solutions with a concentration gradient from 0.5-3.0 μg mL⁻¹ in DMSO/water (v/v, 1/99) were prepared, and the absorbance spectra from 300-500 nm were recorded.

Synthesis of PC₂₀-MOFs-FA

2 mg FA was dissolved into 10 mL DMF solution containing 5 mg PC₂₀-MOFs. The homogeneously dispersed suspension was stirred and reacted at room temperature for 12 h, and then washed with fresh DMF three times to remove uncoordinated FA.³ To determine the content of FA modified on the surface of MOF NPs, the supernatant after the first centrifugation was collected and diluted to 1/20. The UV-vis absorption spectrum of the characteristic peak at 280 nm was measured, and the content of FA was calculated to be 0.31 $\mu\text{M mg}^{-1}$ via the standard linear calibration curve of FA.

***In vitro* stability assay**

10 mL saline and DMEM (10%FBS) were mixed with 2 mg PC₂₀-MOFs-FA respectively to obtain a suspension of PC₂₀-MOFs-FA with a concentration of 200 $\mu\text{g mL}^{-1}$. After the samples were incubated at 37 °C for 12 h, 24 h, 48 h, 72 h and 96 h, the size and zeta potential of the samples were measured by DLS, respectively.

Photothermal effects of PC₂₀-MOFs-FA

Aqueous dispersions of PC₂₀-MOFs-FA NPs with different concentrations (0, 50, 100, 150, 200 $\mu\text{g mL}^{-1}$) were prepared. In EP tubes, the sample (200 μL) was irradiated with 808 nm near infrared laser (1 W cm^{-2}) for 3 min, and the temperature was monitored every ten seconds by a thermal infrared camera. As described above, PC₂₀-MOFs-FA (200 $\mu\text{g mL}^{-1}$) was irradiated under 808 nm near-infrared laser at different power (0.5, 0.75, 1, 2 W cm^{-2}) for 3 min to evaluate the photothermal effect of the nanoparticles. The heating time and natural cooling time of PC₂₀-MOFs-FA after laser irradiation were recorded, and the photothermal conversion efficiency was calculated according to the previous literature.⁴ The calculation formula is as follow:

$$\eta = \frac{hA(\Delta T_{\text{max,min}} - \Delta T_{\text{max,H}_2\text{O}})}{I(1 - 10^{-A808})}, \quad \tau_s = \frac{\sum_i m_i C_{p,i}}{hA}$$

$\Delta T_{\text{max,min}}$, is the temperature change of PC₂₀-MOFs-FA aqueous dispersion, $\Delta T_{\text{max,H}_2\text{O}}$, is the temperature change of water, I is the power density of the laser, $A808$ is the

absorption intensity of PC₂₀-MOFs-FA at 808 nm, m is the mass, C_p is the specific heat capacity, and τ_s can be calculated by the linear relationship between time and $-\ln(\theta)$.

Photodynamic effects of PC₂₀-MOFs-FA

10 μ L DMSO solution of DPBF (3.5 μ g mL⁻¹) was added to PC₂₀-MOFs-FA aqueous dispersion (1 mL, 10 μ g mL⁻¹) and ultrasonically dispersed. After irradiation with 660 nm laser (0.1 W cm⁻²) or 808 nm laser (1 W cm⁻²) for different times (0, 1, 2, 4, 6, 8, 10 min), the absorbance at 415 nm of samples were measured by UV-Vis spectrophotometer. The ROS generation of PC-MOFs was characterized by measuring the absorbance decrease of DPBF at 415 nm. The relative ROS production was determined as I/I_0 (I_0 refers to the absorbance intensity of DPBF at 0 min).

Cytotoxicity assessment

L929, HepG2, 4T1, and CT26 cells were used to evaluate cytotoxicity of NPs. Briefly, L929, HepG2, 4T1, and CT26 cells were incubated in 96-well plates for 24 h and then incubated with different concentrations (0, 25, 50, 100, 150, 200 μ g mL⁻¹) of PC₂₀-MOFs-FA for 24 h. 3-(4,5-dimethylthiazol-2-yl)-2,5-diphenyltetrazolium bromide (MTT) assays were used to detect the cell viability.

Hemolysis assay

The blood of BALB / c mouse was collected by anticoagulation tube and washed with PBS (300 rpm, 5 min) by centrifugation to obtain fresh red blood cells (RBCs) suspension. 4% RBCs (0.25 mL) suspension was added into PBS (0.25 mL) containing different concentrations of PC₂₀-MOFs-FA (0, 20, 40, 60, 80, 160 μ g mL⁻¹), of which 0 μ g mL⁻¹ was used as the negative control group, and deionized water (0.25 mL) was added to RBCs suspension (0.25 mL) as positive control group. Finally, all of samples were incubated at 37 °C for 6 h, and centrifuged to collect supernatant for detection of hemolysis. The absorbance of each group at 540 nm was detected by UV-vis spectrophotometer, and the hemolysis rate of PC₂₀-MOFs-FA was calculated as follow:

Hemolysis % = [(sample absorbance – negative control absorbance) / (positive control absorbance – negative control absorbance)] × 100%.

***In vivo* biocompatibility.**

In vivo biocompatibility of PC₂₀-MOFs-FA was evaluated by hematoxylin and eosin (H&E) staining of organs and serum biochemistry test. The PC₂₀-MOFs-FA (15 mg kg⁻¹) was administered to each mouse by intravenous injection, and three healthy BALB/c mice were selected as the control group. After 14 days, mice were anesthetized to collect blood. Blood supernatant harvested via centrifugation was used to analyze the serum biochemistry parameters. Three hepatic function indicators (ALT, AST, ALB), two kidney function indicators (BUN, CR) were measured. Next, the mice were sacrificed, and the main organs (heart, liver, spleen, lung and kidney) were collected for H&E staining. These analyses were provided by Wuhan Baiqiandu biotechnology Co., LTD.

Cellular uptake

After incubating 4T1 cells in a glass-bottomed dish for 24 h, they were incubated with PC₂₀-MOFs-FA (100 μg mL⁻¹) for 2h, 4h, 8h, 12h, and 24h. The cells were then washed three times with PBS, and DAPI were used to stain the cell nuclei. Finally, intracellular fluorescence intensity was monitored by laser confocal microscopy.

***In vitro* PDT and PTT experiments**

After inoculating 4T1 cells into a 96-well plate and culturing for 24 h, various concentrations of PC₂₀-MOFs-FA (0, 25, 50, 100, 150 μg mL⁻¹) was added and incubated with cells for 8 h. Then, 660 nm laser (0.1 W cm⁻², 5 min) and 808 nm laser (1 W cm⁻², 5 min) were used to irradiate cells in corresponding group. After additional 24 h incubation, the cell viability was measured by MTT assays.

Calcein-AM/PI Double Staining

Cells were seeded in a 24-well plate and incubated 24 h in a CO₂ incubator. After removal of the culture medium, PC₂₀-MOFs-FA (100 μg mL⁻¹) was added and incubated with cells for 8 h. Then, 660 nm laser (0.1 W cm⁻², 5 min) and 808 nm laser (1 W cm⁻², 5 min) were used to irradiate cells in the corresponding group. The cells were incubated at 37 °C for another 4 hours, washed twice with PBS and stained with Calcein-AM (500 μL, 2 μM) and PI (500 μL, 4.5 μM) for 15 min. Finally, the cells were washed with PBS twice carefully, and imaged with a laser scanning confocal microscope. The green images of living cells were excited by 488 nm light, and the emission wavelength range was collected at 520 ± 20 nm. The red images of dead cells were excited by 514 nm light, and the emission wavelength range was collected at 640 ± 20 nm.

Construction of 4T1 tumor-bearing mice

Female BALB/c mice (16-18 g) were purchased from Beijing Weitong Lihua Experimental Animal Technology Co., Ltd. All animal experiments were carried out in accordance with China's Laboratory Animal Management Regulations and were approved by the Laboratory Animal Management and Use Committee of Wuhan University. After the mice were adaptively fed for 1 week, 5 × 10⁶ 4T1 cells were injected subcutaneously into the right hip joint of the mice. After tumor volume of mice reached 80 mm³ in 2-3 weeks, the experimental 4T1 tumor-bearing mice model were obtained. The formula for calculating tumor volume is as follows: tumor volume = (tumor width)² * tumor length / 2.

***In vivo* multi-modal imaging**

The near-infrared fluorescence imaging system was used to record the enrichment of materials in tumors after different treatments. 808 nm (90 mW cm⁻²) laser was used as the excitation light. The emitted light was filtered through an 880 nm filter and the InGaAs camera was used to collect the fluorescence signal. PC₂₀-MOFs-FA (15 mg kg⁻¹) and PC₂₀-MOFs (15 mg kg⁻¹) were injected intravenously into 4T1 tumor-bearing mice, and NIRF images were collected at different times (2 h, 4 h, 8 h, 12 h, 24 h, 48

h). Similarly, 4T1 tumor-bearing mice injected with PC₂₀-MOFs-FA (15 mg kg⁻¹) were used for photoacoustic imaging (PAI), and the PA signal at 0 h, 6 h, and 24 h post injection was captured by a high-resolution PAI instrument. Moreover, PC₂₀-MOFs-FA (15 mg kg⁻¹) and the same amount of PBS were intravenously injected into 4T1 tumor-bearing mice. 4 h later, the photothermal imaging system was used to detect the heating effect of laser irradiation at tumor site.

***In vivo* phototherapy**

When the tumors of 4T1 tumor-bearing mice reached approximately 80 mm³, the mice were randomly divided into 1-6 groups (n = 4) with treatments of: 1) PC₂₀-MOFs-FA + 808 nm + 660 nm; 2) PC₂₀-MOFs-FA + 808 nm; 3) PC₂₀-MOFs-FA + 660 nm; 4) PC₂₀-MOFs-FA; 5) PBS + 808 nm + 660 nm; 6) PBS. PC₂₀-MOFs-FA (15 mg kg⁻¹) was injected intravenously into 4T1 tumor-bearing mice as treatment groups and PBS as the control group. It was determined by trimodal imaging that PC₂₀-MOFs-FA reached the maximum enrichment in tumor tissue 24 h after administration. At 24 h post-injection, the different treatment groups were irradiated with 660 nm laser (0.2 W cm⁻², 5 min) or 808 nm laser (1 W cm⁻², 5 min), respectively. The tumor volume and body weight of the mice were measured every other day. After 21 days, the mice in each group were euthanized, and the tumor and main organs were sectioned.

Statistical analysis

The experimental data are expressed as mean ± standard deviation (mean ± SD), and two-tailed student's t test is used to compare the two groups. * P < 0.05, ** P < 0.01, and *** P < 0.001 indicated statistical difference.

Table 1. Recipes and particle sizes in the self-assembly of PC_X-MOFs

Sample	H ₂ TCPP (mg)	ZrOCl ₂ ·8H ₂ O (mg)	BA (mg)	Cypate (mg)	Z-average (nm) ^①	PDI ^②
PCN-224	5	15	140	0	131.4 ± 0.7 nm	0.092
PC ₅ ^③ -MOFs	4	15	140	5	136.4 ± 0.4 nm	0.082
PC ₁₀ -MOFs	4	15	140	10	128.1 ± 1.2 nm	0.077
PC ₂₀ -MOFs	4	15	140	20	127.8 ± 0.4 nm	0.069
PC ₃₀ -MOFs	4	15	140	30	124.8 ± 1.5 nm	0.025
PC ₄₀ -MOFs	4	15	140	40	272.7 ± 7.5 nm	0.421

① Hydrodynamic diameter measured by dynamic light scattering in DMF. ②

Polydispersity index of the particle size. ③ The amount of cypate added to the one-pot synthesis.

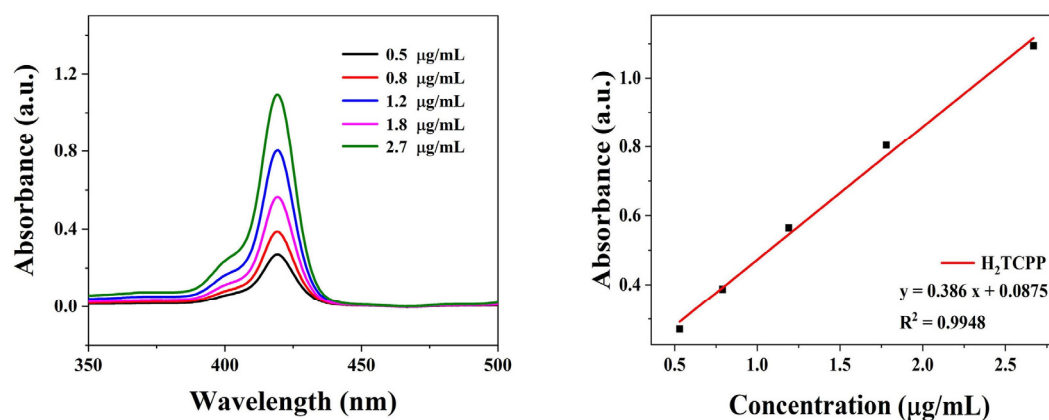


Fig. S1. UV-Vis spectrum and the standard curve of H₂TCPP from 0.5-2.7 µg mL⁻¹.

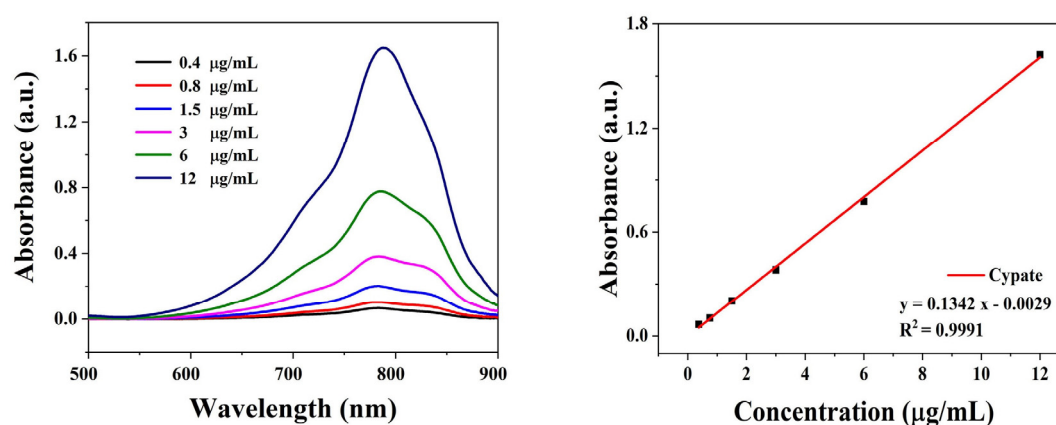


Fig. S2. UV-Vis spectrum and the standard curve of cypate from 0.4-12 µg mL⁻¹.

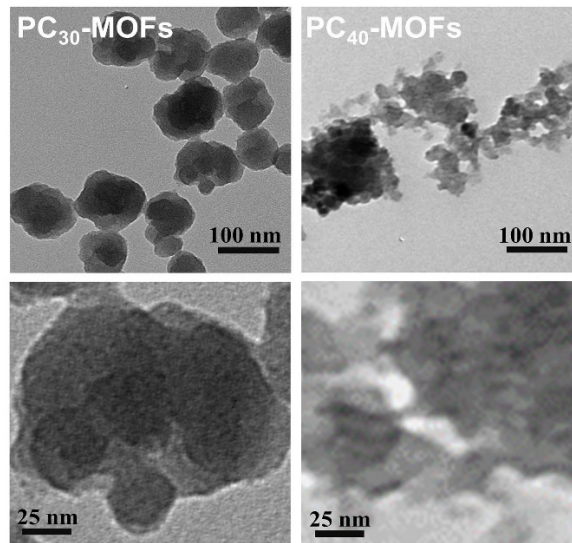


Fig. S3. TEM images of PC₃₀-MOFs and PC₄₀-MOFs NPs.

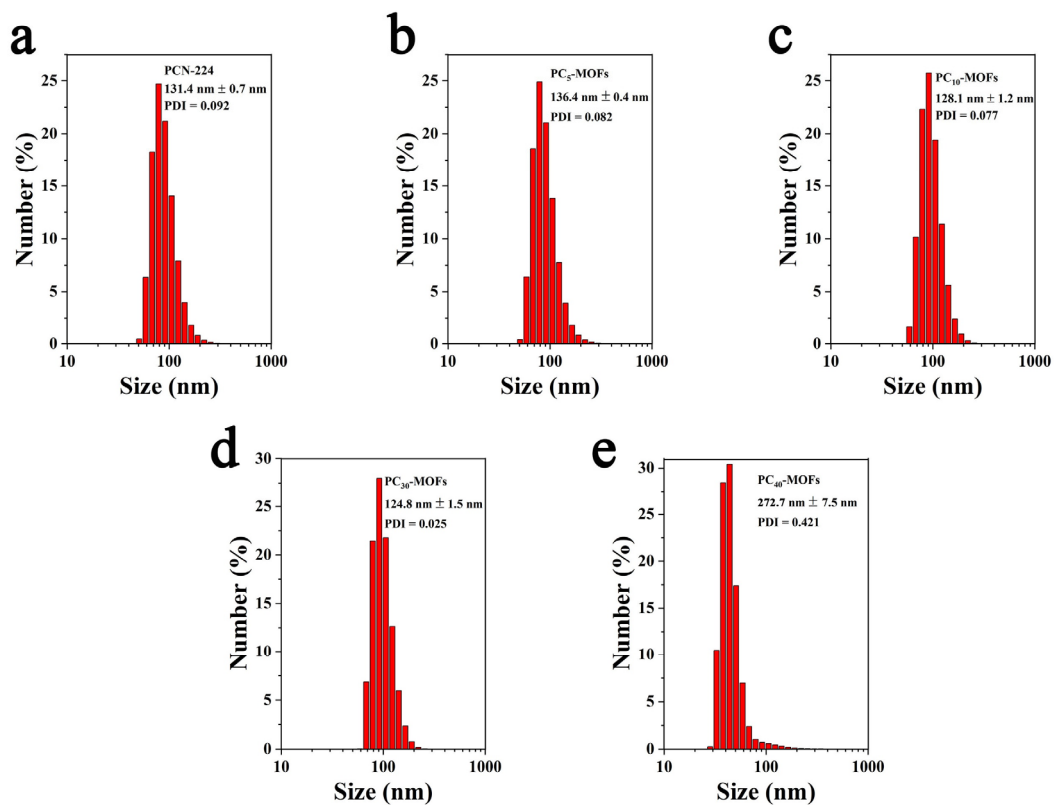


Fig. S4. Dynamic light scattering results for (a) PCN-224, (b) PC₅-MOFs-FA, (c) PC₁₀-MOFs-FA, (d) PC₃₀-MOFs-FA, and (e) PC₄₀-MOFs-FA.

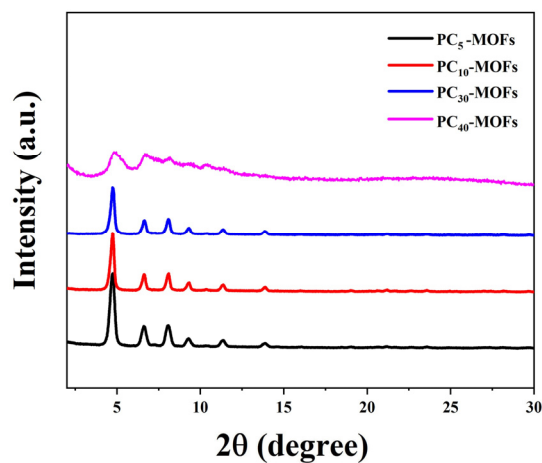


Fig. S5. PXRD patterns of PC₅-MOFs, PC₁₀-MOFs, PC₃₀-MOFs, and PC₄₀-MOFs NPs.

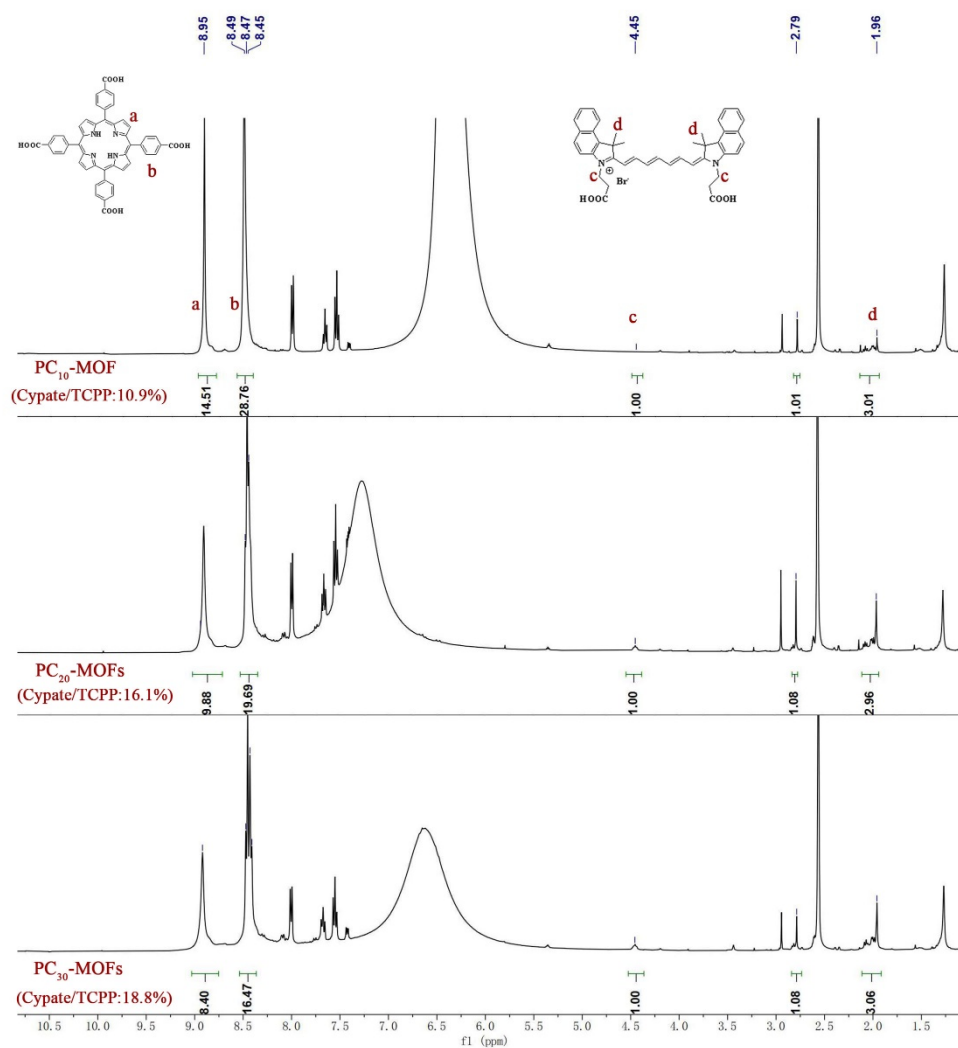


Fig. S6. 400 MHz ¹H-NMR spectra of dissolved PC₁₀-MOFs NPs, PC₂₀-MOFs NPs, PC₃₀-MOFs in trifluoroacetic acid-*d* (TFA-*d*)/DMSO-*d*₆ (v/v, 1/20).

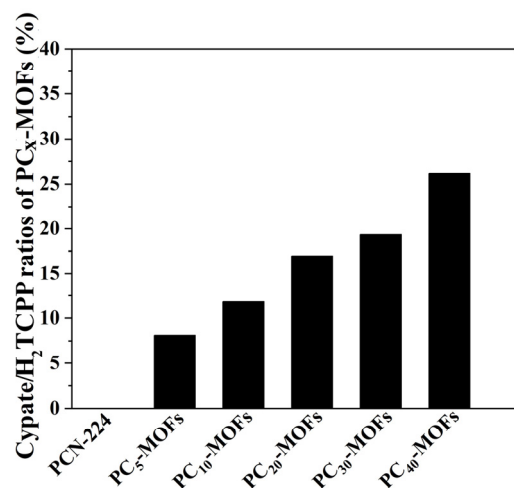


Fig. S7. The ratio of cypate/H₂TCPP in PC_x-MOFs determined from standard curves.

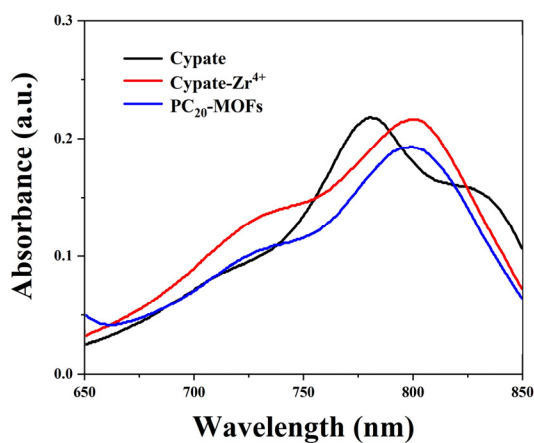


Fig. S8. UV-Vis spectrum of cypate alone, cypate-Zr⁴⁺ complexes and PC₂₀-MOFs in DMF.

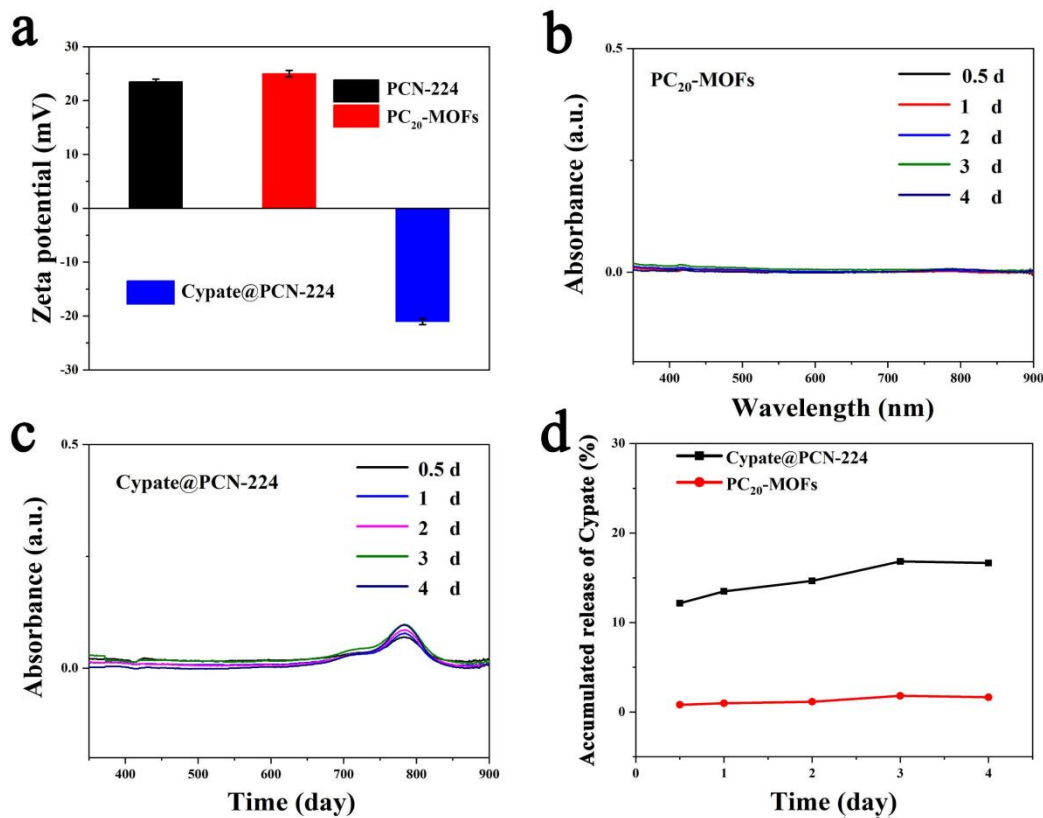


Fig. S9. a) Zeta potential of PCN-224, PC₂₀-MOFs and cypate@PCN-224. b) UV-Vis spectrum of methanol dialysate after dialysis of PC₂₀-MOFs. c) UV-Vis spectrum of methanol dialysate after dialysis of cypate@PCN-224. d) The corresponding quantitative analysis of cypate leaking by UV-Vis spectra.

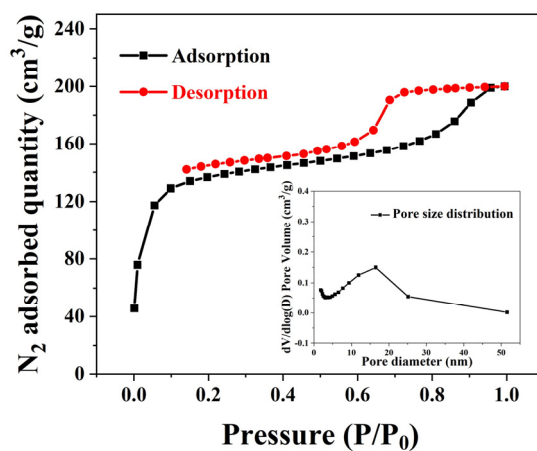


Fig. S10. The nitrogen adsorption isotherm of PC₂₀-MOFs.

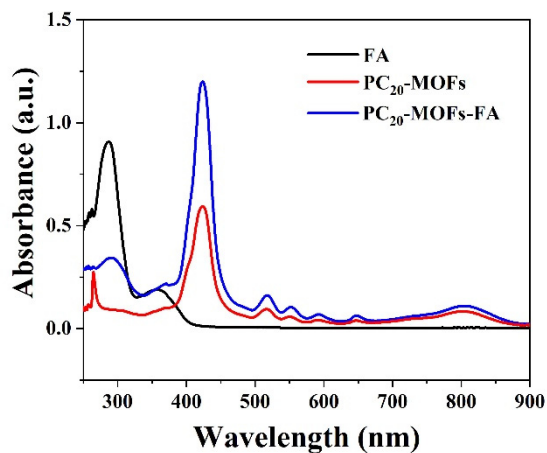


Fig. S11. UV-Vis spectra of PC₂₀-MOFs, PC₂₀-MOFs-FA, and FA.

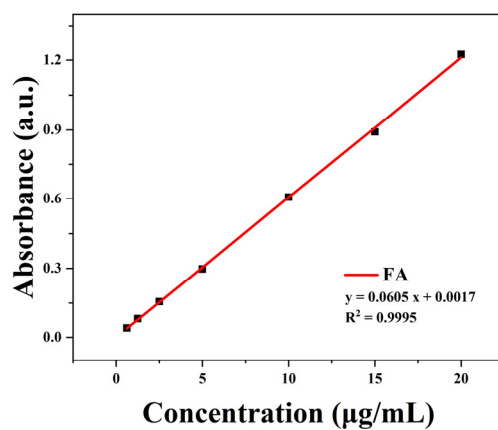


Fig. S12. Calibration curve of folic acid in DMF at 280 nm.

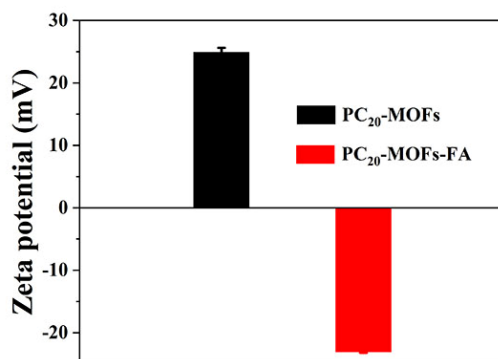


Fig. S13. Zeta potential of PC₂₀-MOFs and PC₂₀-MOFs-FA NPs.

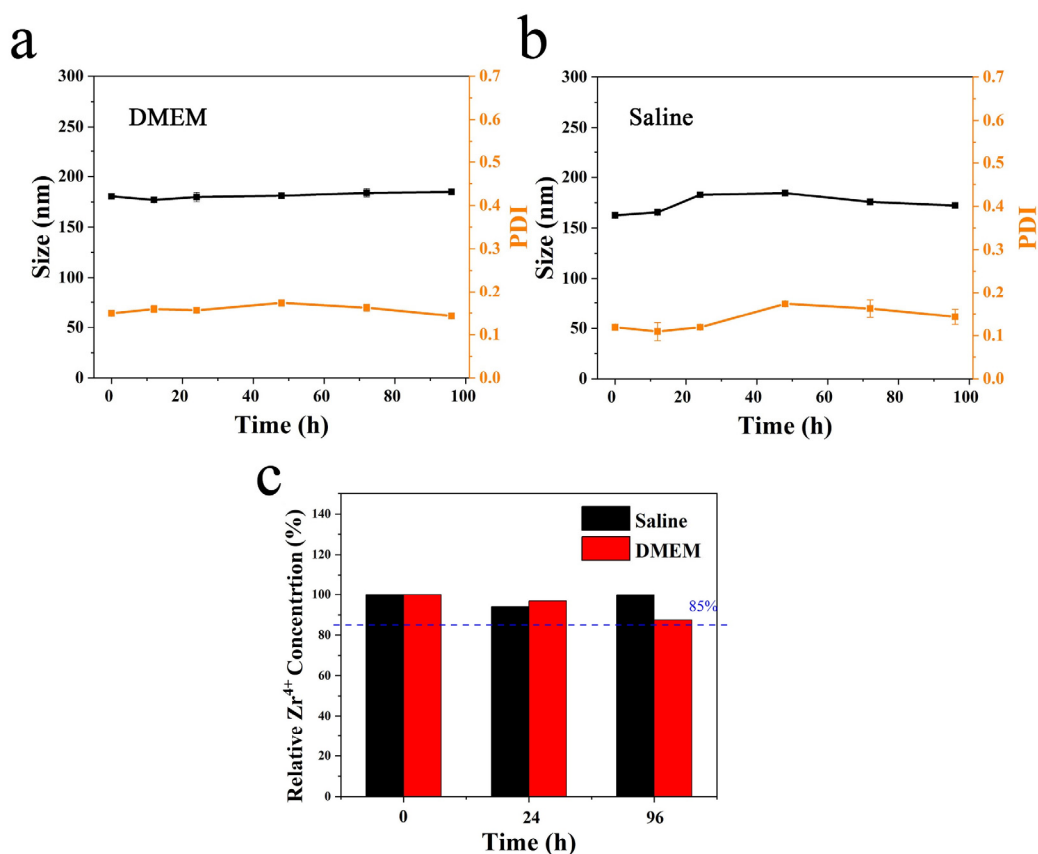


Fig. S14. a, b) Changes in the hydrodynamic particle size and PDI of PC₂₀-MOFs-FA in cell culture medium (DMEM + 10% FBS) and saline. c) Content of Zr⁴⁺ in PC₂₀-MOFs NPs after co-incubation with saline and cell culture medium as determined by ICP-MS.

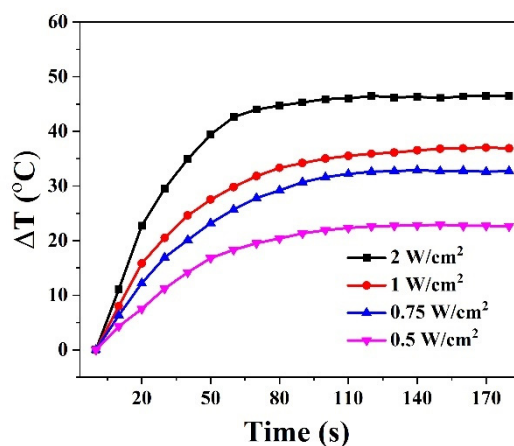


Fig. 15. The temperature changes of PC₂₀-MOFs-FA aqueous suspension (200 $\mu\text{g mL}^{-1}$) under different powers of 808 nm laser irradiation.

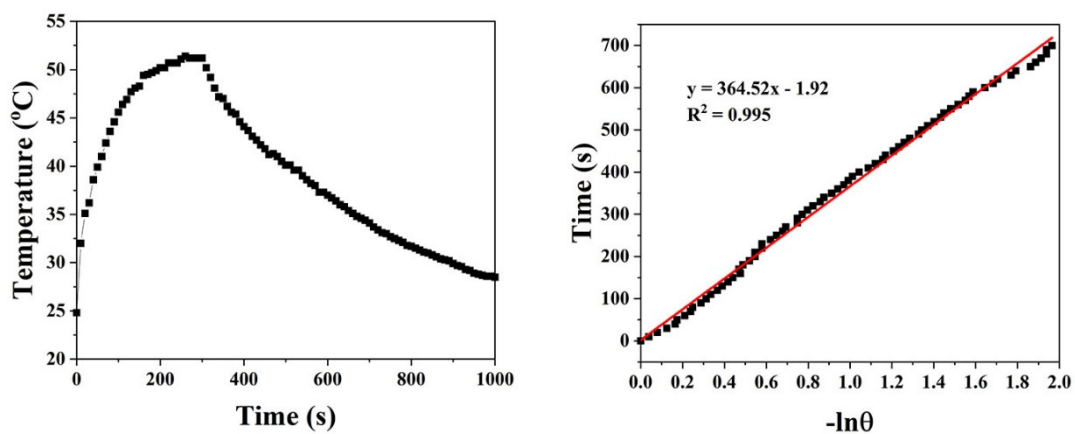


Fig. S16. The heating/cooling curve of PC₂₀-MOFs-FA aqueous dispersion under 808 nm laser (1 W cm^{-2}) and linear relationship between $-\ln\theta$ and time during cooling.

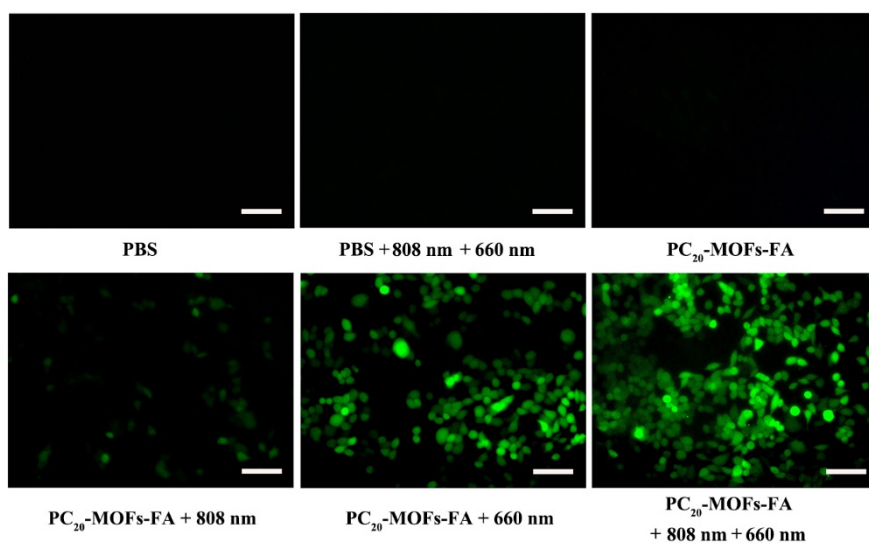


Fig. S17. Fluorescent inverted microscope images of ROS by 4T1 cells detected with DCFH-DA. Scale bar: $100 \mu\text{m}$.

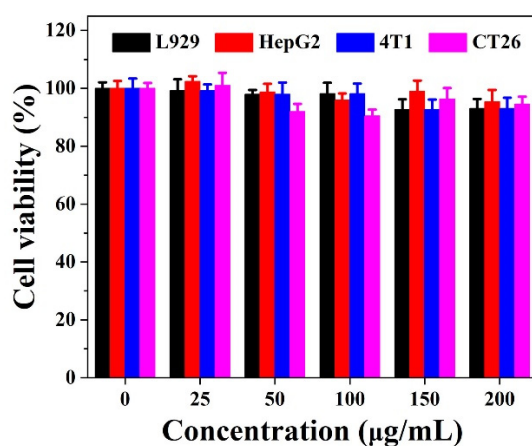


Fig. S18. Cell viability of L929, HepG2, 4T1, and CT26 cells incubated with various concentrations of PC₂₀-MOFs-FA.

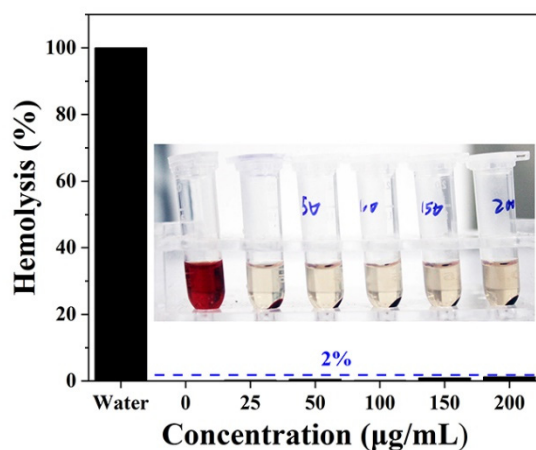


Fig. S19. Image and hemolysis rate of RBCs incubated with different concentrations of PC₂₀-MOFs-FA at 37 °C for 6 h.

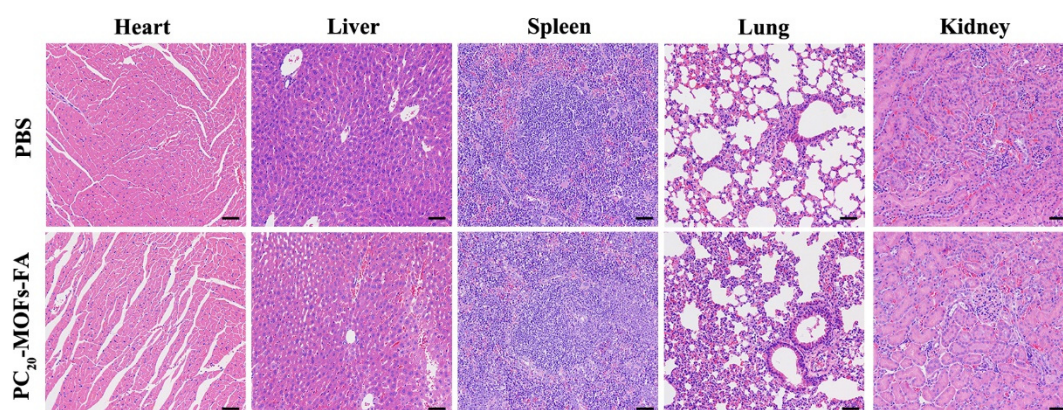


Fig. S20. H&E stained images of major organs treated with PBS or PC₂₀-MOFs-FA administration (15 mg kg⁻¹). Scale bar: 50 µm.

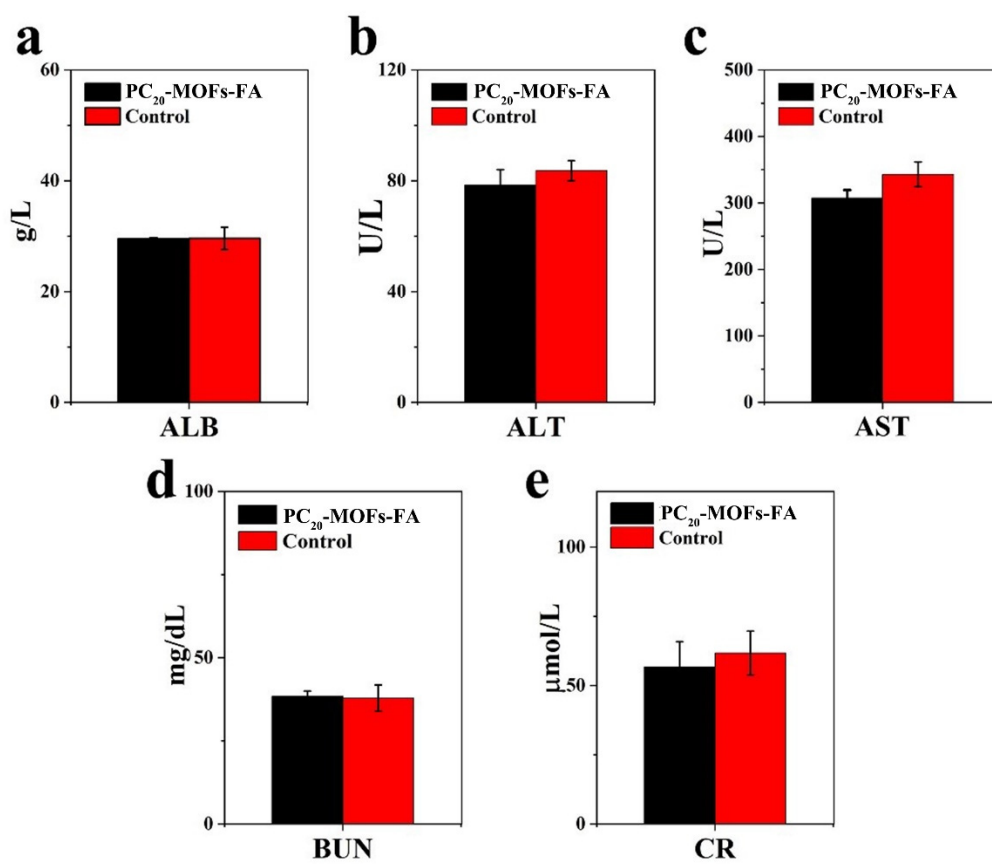


Fig. S21. Serum biochemical indicators of mice treated with PBS or PC₂₀-MOFs-FA (15 mg kg⁻¹).

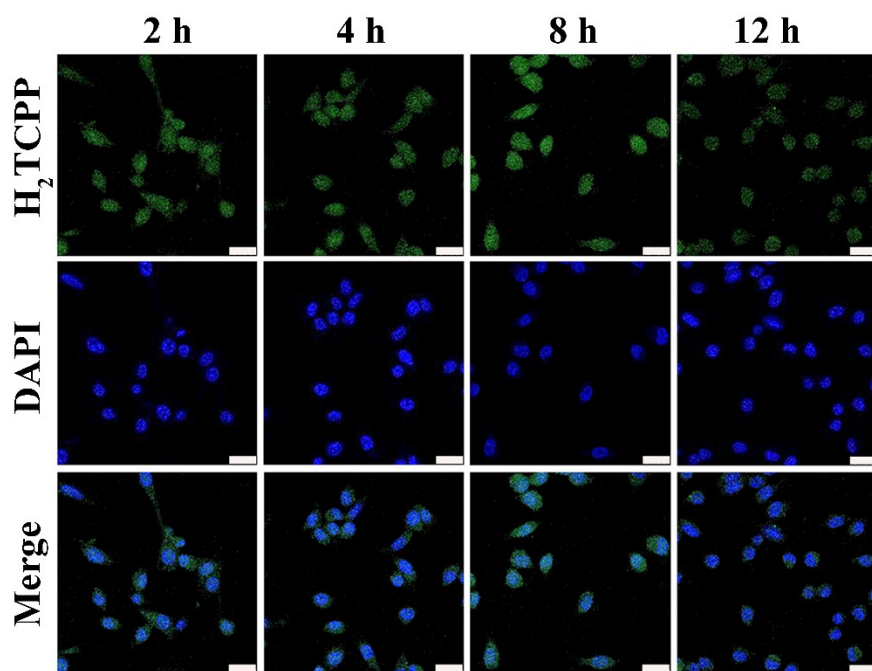


Fig. S22. CLSM images of 4T1 cells incubated with PC₂₀-MOFs-FA for different times. Blue represented FL of DAPI, and green represented FL of H₂TCPP. Scale bar: 25 μm.

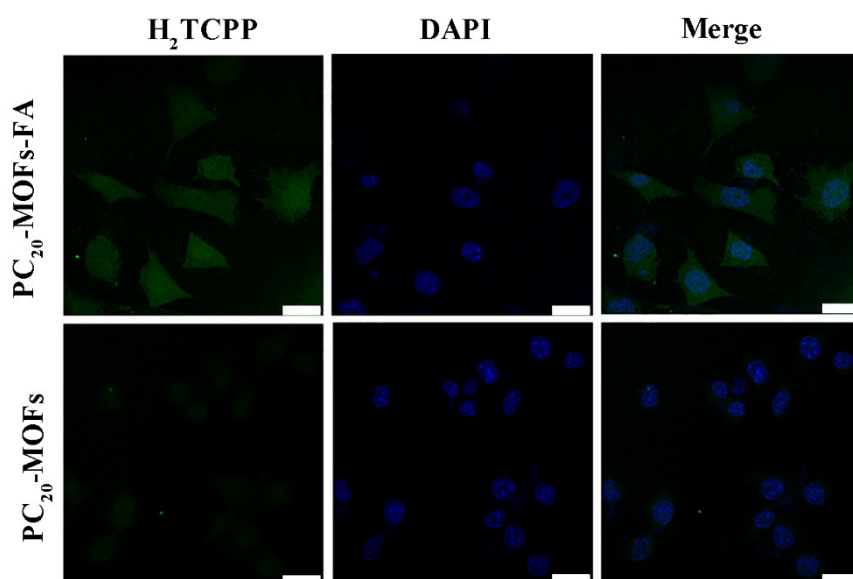


Fig. S23. CLSM images analysis of 4T1 cells after incubated with PC₂₀-MOFs-FA or PC₂₀-MOFs for 8 h. Blue represented FL of DAPI, and green represented FL of H₂TCPP. Scale bar: 25 μm.

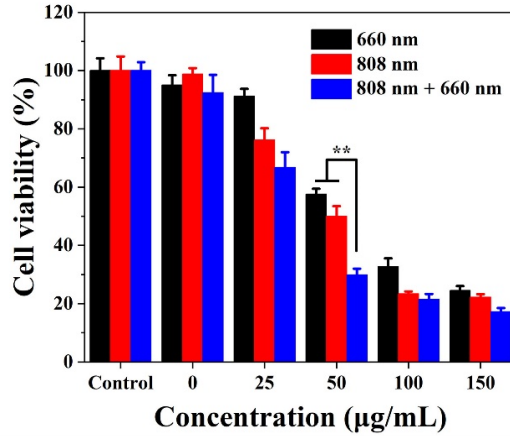


Fig. S24. Cell viability of 4T1 cells under 808/660 nm laser irradiation after incubated with PC₂₀-MOFs-FA. (**p < 0.01).

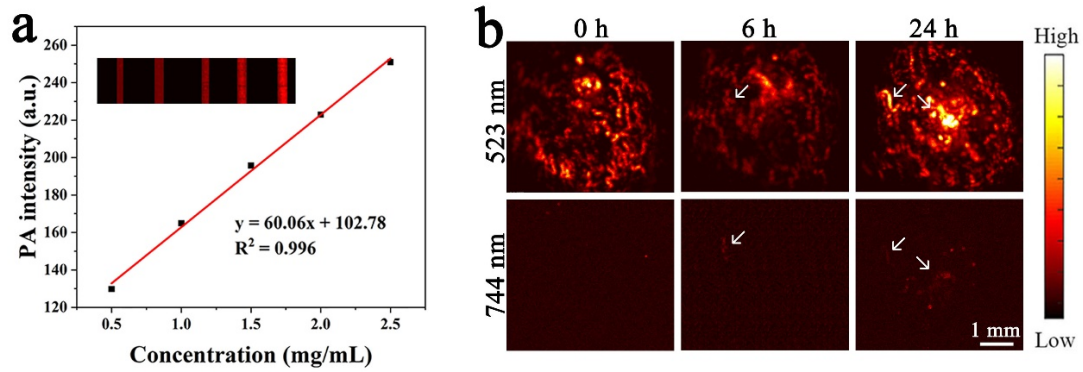


Fig. S25. a) In vitro PA signal versus various concentrations of PC₂₀-MOFs-FA. b) PA images of the tumor area of 4T1 mice before and after IV injection of PC₂₀-MOFs-FA. The signal at 523 nm was tumor blood vessels and the signal at 744 nm was PC₂₀-MOFs-FA.

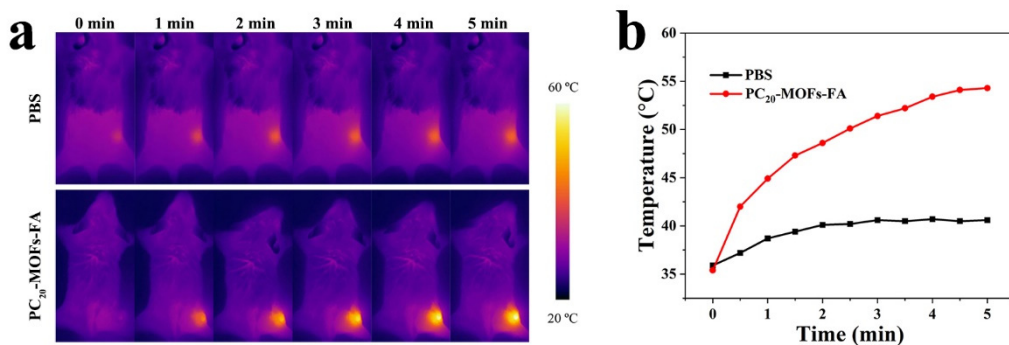


Fig. S26. a) Infrared thermal images and b) temperature changes of tumor area of 4T1 tumor-bearing mice treated with PBS and PC₂₀-MOFs-FA (15 mg kg⁻¹) during 808 nm laser irradiation (5 min, 1 W cm⁻²).

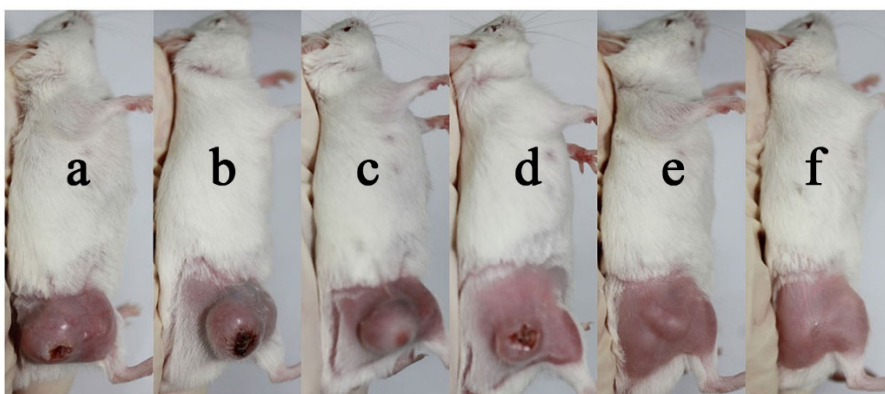


Fig. S27. Photographs of 4T1 tumor-bearing mice 21 days after different treatments (a: PBS, b: PBS + 808 nm + 660 nm, c: PC₂₀-MOFs-FA, d: PC₂₀-MOFs-FA + 660 nm, e: PC₂₀-MOFs-FA + 808 nm, f: PC₂₀-MOFs-FA + 808 nm + 660 nm. (mean \pm SD, n = 4).

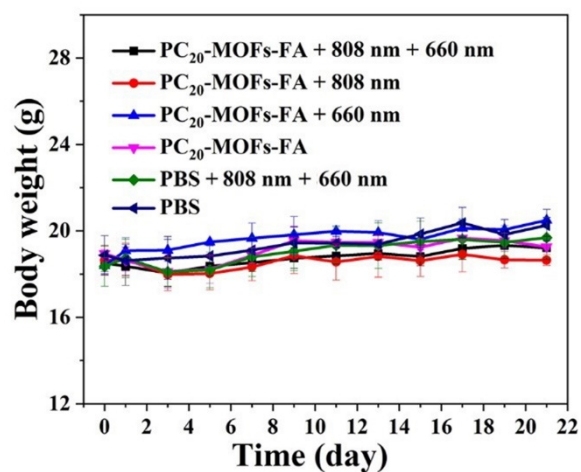


Fig. S28. Body weight changes of mice received different treatments within 21 days.

References

1. S. Yuan, T. F. Liu, D. Feng, J. Tian, K. Wang, J. Qin, Q. Zhang, Y. P. Chen, M. Bosch, L. Zou, S. J. Teat, S. J. Dalgarno and H. C. Zhou, *Chem. Sci.*, 2015, **6**, 3926-3930.
2. P. Yang, Y. Men, Y. Tian, Y. Cao, L. Zhang, X. Yao and W. Yang, *ACS Appl. Mater. Interfaces*, 2019, **11**, 11209-11219.
3. C. Liu, J. Xing, O. U. Akakuru, L. Luo, S. Sun, R. Zou, Z. Yu, Q. Fang and A. Wu, *Nano Lett.*, 2019, **19**, 5674-5682.
4. W. Ren, Y. Yan, L. Zeng, Z. Shi, A. Gong, P. Schaaf, D. Wang, J. Zhao, B. Zou, H. Yu, G. Chen, E. M. Brown and A. Wu, *Adv. Healthc. Mater.*, 2015, **4**, 1526-1536.